Evaluating the Thermal Stability of High Performance Fibers by TGA

Xiaoyan Liu,[1] Weidong Yu[1,2]

[1]College of Textiles, Dong Hua University, Shanghai 200051, People's Republic of China
[2]Wuhan University of Science and Engineering, Wuhan, 430073, People's Republic of China

ABSTRACT: The thermal degradation of eight types of high performance fibers (HPFs) was measured under nitrogen and air atmosphere. The degree of degradation, as measured by weight loss using thermogravimetric analysis (TGA), and the characteristic degradation temperatures were obtained. The kinetics of the thermal degradation has also been analyzed according to the Freeman–carroll method and the activation energies of the HPFs were estimated. The experimental results show that *para*-aramids (Kevlar® 29, 49, 129, and Twaron®2000) have similar thermal stability, but their thermal degradation temperatures and activation energies in air are different from those in nitrogen, which means that the thermostability of the fiber depends not only on its intrinsic structure but also on the atmosphere and temperature of testing environment. Terlon® fiber shows higher degradation temperature as a copolymer of *para*-aramid, and its initial degradation temperature is 476.4°C in air. It can also be found that the PBO (poly(*p*-phenylene benzobisoxazole)) fiber has the highest thermal degradation temperature among the samples tested, but its activation energy is not the highest in both air and nitrogen atmosphere. And the UHMW-PE (ultra high molecular weight polyethylene) fiber has the lowest thermal degradation temperature, and it begins to degrade when the temperature reaches 321.8°C under air atmosphere. © 2005 Wiley Periodicals, Inc. J Appl Polym Sci 99: 937–944, 2006

Key words: fibers; degradation; thermogravimetric analysis (TGA); kinetics; activation energy

INTRODUCTION

In the last few decades, the demand of advanced industries, particularly for the aerospace, has been driving the force on the development and applications of high performance fibers (HPFs) in many fields, such as structural, composite, and reinforced materials. Aromatic thermoplastic polymers offer favorable properties, i.e., excellent thermal and oxidative stability[1,2] and the retention of physical properties[3] at high temperature, which make the materials very suitable for many purposes.[4,5,6,7]

The popular commercial HPFs are Kevlar® fibers, namely *para*-aramids. Because of the high tenacity, modulus, and remarkable thermostability, the fibers are widely used as tire reinforced materials, ropes, cables, and ballistic resistance fabrics, since it was born in Du Pont company in the 1960s.[8,9] Similarly, the other high performance fibers have been introduced in succession, such as polybenzimidazole (PBI) from Celanese (Dallas, TX),[10,11] poly(*p*-phenylene benzobisoxazole) (PBO) from Dow Chemical Co., Ltd. (Midland, MI), and ultra high molecular weight polyethylene (UHMW-PE) from D.S.M. (The Netherlands),[12,13] and so on.

Although the considerable efforts have been devoted to study the HPFs structure,[14,15] thermal properties,[16,17] and their relationship,[18,19] there are few publications on the comparison in their thermal stability and thermal degradation kinetics. Li[20] ever investigated the thermal degradation of Kevlar fiber by high-resolution thermogravimetry and found that the degradation of Kevlar in nitrogen or air occurs in one step. Newell[21] found an activation energy of 76 ± 6 kcal/mol for the thermal initiation of free radicals of PBO fiber during the carbonization process, and the activation energy for graphitization to be 120 ± 17 kcal/mol.

Besides these results, there are less detailed reports about the kinetics of these fibers. Therefore, the characteristic behavior and the kinetics of the thermal degradation for these HPFs are discussed in this paper. Moreover, the thermostable properties of these fibers in air and nitrogen atmosphere are compared because the result tested in air atmosphere can be used to evaluate the oxidation at normal condition, whereas, under the nitrogen atmosphere, the fibers show their native character without the oxidative effect.
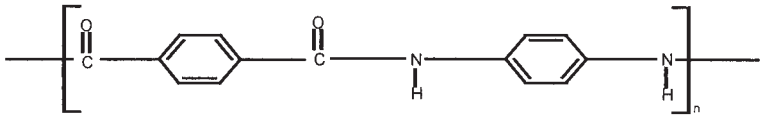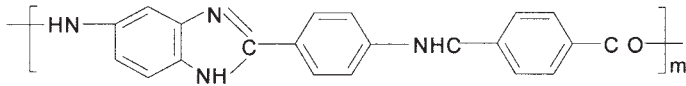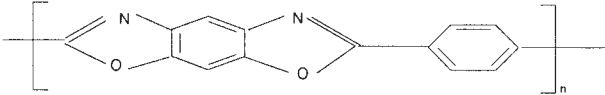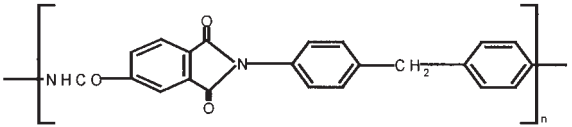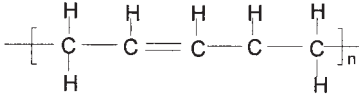
EXPERIMENTAL

Materials

Eight types of high performance fibers were collected, including Kevlar®29, 49, 129, Twaron®2000, Terlon®,

---

Correspondence to: W. Yu (wdyu@dhu.edu.cn).

TABLE I
Sample and Specification

Name	Chemical structure	Manufacturer
Kevlar®29 Kevlar®49 Kevlar®129 Twaron®2000		Du Pont (USA) Du Pont (USA) Du Pont (USA) Akzo (The Netherlands)
Terlon®		Research Center of Synthetic Fiber (Russia)
PBO(AS)		TORY (Japan)
Kermel®		Kermel (France)
Dyneema®SK65		D.S.M. (The Netherlands)

PBO (AS), Kermel®, and Dyneema®SK65 (UHMW-PE). Their specifications are listed in Table I.

Testing conditions

Thermal degradations of these HPFs were performed in a Perkin–Elmer TGA 7 (Thermogravimetric Analysis) from the Perkin–Elmer, Inc. The temperature calibration of the thermobalance was made according to the procedure reported in the user's manual of the equipment.[22]

The thermal scanning mode ranges from 50 to 800°C at a programming heating rate of 20°C/min in both nitrogen and air atmosphere with a gas flow of 20 mL/min.

The thermal and thermo-oxidative stability of the eight high performance fibers were studied by thermogravimetric measurements (TG) in air and nitrogen atmosphere.

Calculation

Each of the samples was controlled within 5–6 mg in primary weight and held in an alumina crucible, and then the loss of the sample weight (W) was measured under a temperature program. The thermogravimetric (TG) and differential thermogravimetric (DTG) curves were recorded and displayed simultaneously during the measurement. The loss of weight, α, is equal to $(W_0-W)/W_0$, where W_0 and W represent the weight of the sample at the starting point and during the scanning, respectively. The residual percentage of the weight, m (%), equals to $(1-\alpha) \times 100$ and is a function of temperature, T (°C), that is a thermogravimetric curve (TG), or "m (%)–T" curve.

DTG is the differential of TG curve, which indicates the changing rate of m to temperature. The point for the quickest degradation temperature can be found from the bottom-peak point of the DTG curve.

Regarding to the temperature parameters, they are the initial temperature of decomposition (T_i), the temperature of half decomposition ($T_{1/2}$), and the temperature at the maximum rate of weight loss (T_p), respectively. These parameters are defined in this present paper and obtained from the measured TG and DTG curves, which are useful for the analysis of the thermodegradation dynamics to find the activation energy (E) of the eight fibers. The initial degradation temperature (T_i) occurs at the point given by the angle bisector of the tangent at the origin, with the tangent having the sharp shape passing the intersection to TG or DTG curve, as illustrated in Figure 1. For simplification, we take only the point (T_i) from TG curve in this paper. The temperature of half decomposition, $T_{1/2}$, is taken as the temperature where the weight loss reaches the 50% of its total reduction during the degradation. The T_p value is the temperature of the lowest DTG peaks. The schematic method is shown in Figure 1.
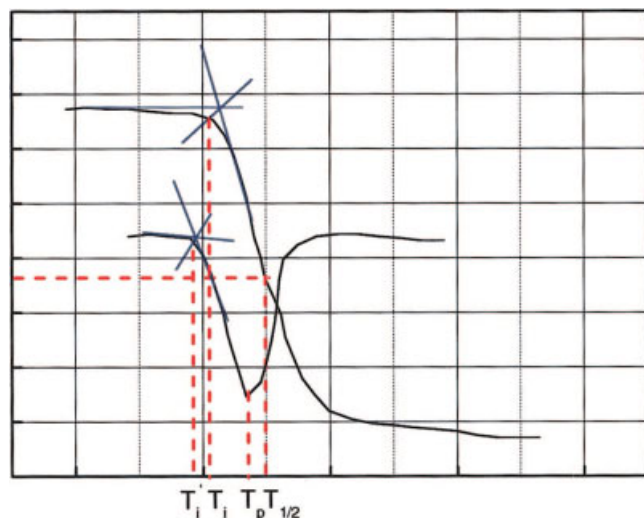
Figure 1 The schematic diagram to find T_i, $T_{1/2}$ and T_p. [Color figure can be viewed in the online issue, which is available at www.interscience.wiley.com.]

RESULTS AND DISCUSSION

Degradation under nitrogen flow

The dynamic TG curves and the corresponding DTG curves are illustrated in Figure 2.

The measured curves of homopolymer *para*-aramids, Kevlar®29, 49, 129, and Twaron®2000 have the same shape. However, the degradation behavior of the Terlon® fiber is different from the Kevlar® fibers because it belongs to the *para*-aramid of copolymer, the heterocyclic chain segment is less than 15%. The wider peak zone of the DTG curve shows that the degradation of Terlon® fibers has a stable mild mechanism not as that of the other seven tested samples. The TG and DTG curves of Kermel®, PBO, and UHMW-PE fibers are quite similar to the Kevlar's in general shape, but the characteristic temperatures are different from each other, as shown in Table II.

The measured results, thermally treated in nitrogen atmosphere, indicate that the initial degradation temperature of the PBO is the highest ($T_i = 556.5°C$); that of the UHMW-PE is the lowest ($T_i = 355.9°C$); and all the *para*-aramid fibers are close. For T_p and $T_{1/2}$, the order of the three Kevlar® fibers is the same as their T_i sequence, i.e., Kevlar®29>Kevlar®49>Kevlar®129.

The PBO, Terlon®, and Kermel® samples show higher degradation temperature because of their heterocyclic rigid conformation of the molecules,[23,24] and Kevlar® corresponds to the *N*-acylamide structure of its backbone.[25] Compared with the other tested samples, the chain of UHMW-PE fiber is flexible and the double bond is unstable, and so its thermal property is inferior to the other tested fibers.

At the same time, it can be found obviously from the DTG curves of the *para*-aramids in Figure 2 that there
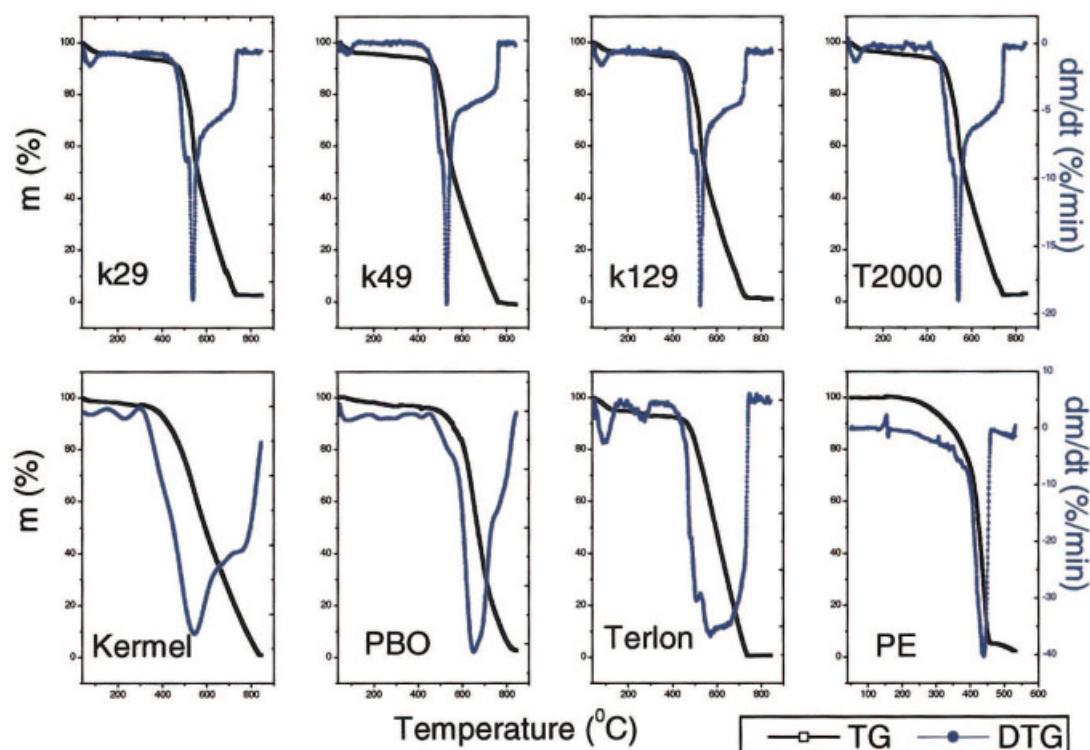
Figure 2 TG and DTG curves under nitrogen flow. [Color figure can be viewed in the online issue, which is available at www.interscience.wiley.com.]

TABLE II
The Characteristic Degradation Temperatures

Atmosphere	Degradation Temperature	Sample							
		K29	K49	K129	T2000	PBO	Terlon®	Kermel®	PE
Air	T_i'	449.1	451.0	437.1	432.2	515.1	476.4	371.5	321.8
	T_p'	502.6	499.0	489.2	494.0	610.1	550.1	501.9	387.8
	$T_{1/2}'$	515.3	510.0	498.6	510.8	615.1	587.1	501.4	391.2
N_2	T_i	480.0	474.7	464.2	472.2	556.5	473.5	411.2	355.9
	T_p	541.0	531.8	527.8	542.9	648.2	568.1	553.0	441.3
	$T_{1/2}$	562.7	561.4	551.2	568.6	670.7	596.7	595.1	427.4

The characteristic degradation temperatures of eight samples are obtained according to the Figure 2's method. T_i (T_i') is the initial temperature of decomposition in nitrogen (air), T_p (T_p') is the temperature at the maximum rate of weight loss in nitrogen (air), and $T_{1/2}$ ($T_{1/2}'$) is the temperature of half decomposition in nitrogen (air).

exists a small peak at about 100°C, which was due to water evaporation in the samples.

Degradation under air flow

For the three Kevlar® fibers and the Twaron® fiber, the TG and DTG curves are similar in shape, seen in Figures 3(a) and 3(c), which means that the thermodegradation is the same. For the other four samples, i.e., Kermel®, PBO, Terlon®, and UHMW-PE, the TG and DTG curves are obviously different, not only in the initial and the end stage, but also during the degradation procedure under the heating programming, as shown in Figures 3(b) and 3(d).

For the typical temperatures of these samples in air atmosphere, they were also derived from Figure 3 by means of the schematic method mentioned in Figure 1, and are listed in Table II.

The initial degradation temperature in air, T_i', is in the range of 321.8–515.1°C and in the order of PBO> Terlon®> Kevlar®49> Kevlar®29> Kevlar®129> Twaron®> Kermel®> UHMW-PE. The sequence for T_p' and $T_{1/2}'$ of the eight fibers is still that PBO and Terlon® are the first two and UHMW-PE is the last one. There is a little difference among the five others, especially for the Kermel® fiber, that T_p' and $T_{1/2}'$ become high.

Comparison of the characteristic degradation temperatures

Comparing the TG and DTG curves in Figure 2 and Figure 3, it can be found that the degradation curves of the eight samples are close to each other in shape under the two atmosphere conditions. The differences for the samples between in air and nitrogen are the
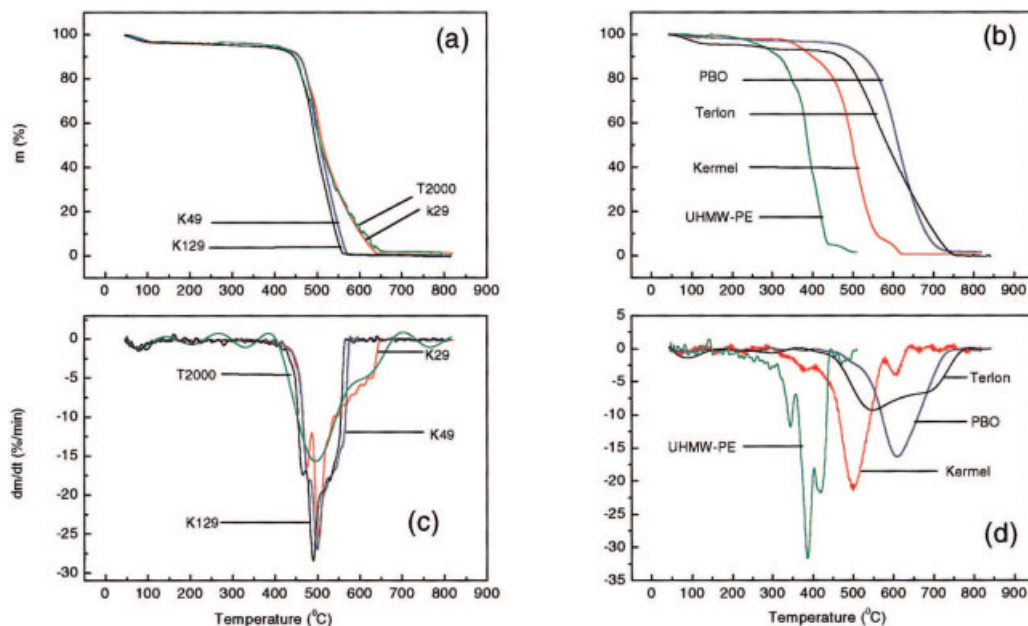

Figure 3 TG and DTG curves in air. [Color figure can be viewed in the online issue, which is available at www.interscience.wiley.com.]
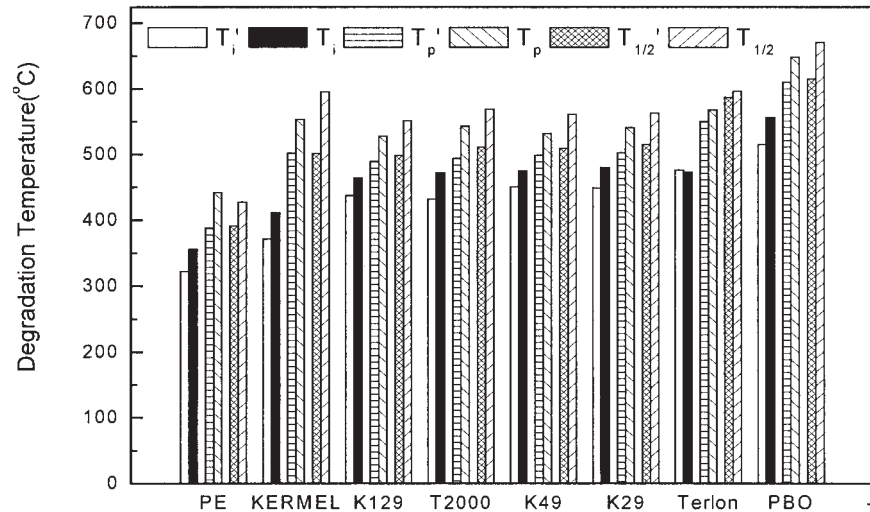
Figure 4 The schematic comparison of the typical degradation temperatures of the eight fibers.

typical temperatures and the residue rate of the decomposition. The explanation on the initial decrease of the sample mass and the relatively quick degradation is more complex in air than in nitrogen atmosphere, mainly because of various oxidation reactions.[26]

According to the typical temperature, T_i, T_p, and $T_{1/2}$, the characteristics of these samples under air and nitrogen atmosphere are compared as shown in Table II.

From the Table II, it can be found that all of the degradation temperatures in nitrogen are higher than those in air atmosphere except for the T_i' of Terlon® fiber. The difference between T_i values is about 30°C, that between T_p values is about 40°C, and that between $T_{1/2}$ values is 50°C or more. However, the degradation temperatures of the Terlon® fiber are approximately the same whether in air or in nitrogen, that is to say, there is less difference of thermostability between air and N_2 atmosphere for the Terlon® fibers. The results maybe thanks for its special structure and synthesis process, so that it has superior thermal resistant property in various atmosphere.

The comparison for the typical temperatures of these samples is illustrated in Figure 4, where the column height represents the value of the typical temperature. According to the analysis of Figure 4, it can be concluded that the PBO sample is the highest in temperature. The figure indicates that PBO is the best in thermal stability, the following is the Terlon®, and then three Kevlar® samples, Twaron® and Kermel®, and the last is UHMW-PE fiber.

It is obvious that the characteristic temperature of the PBO degradation is about 100°C higher than that of the Kevlar® samples whether in air or nitrogen atmosphere. In the tested *para*-aramid fibers, Terlon® is also one of the most thermostable fibers though its typical temperatures are lower than those of PBO.

PBO fiber shows the most stable thermal property of the tested samples, which is associated with its production procedure where no isomer occurs.

Based on the influencing quantity of the typical degradation temperatures, i.e., T_i, T_p, and $T_{1/2}$ on thermal degradation in end usage, a collecting temperature parameter Tc and the influencing factors C_j, are adopted and defined to evaluate thermal stability comprehensively and directly. The formula to calculate Tc is

$$T_c = \frac{C_1 T_i + C_2 T_p + C_3 T_{1/2}}{\sum C_j} \qquad (1)$$

where C_j represents the influencing factor according to the effect of each typical degradation temperature on fiber degradation, i.e., the weight coefficient of the typical temperatures, $j = 1,2,3$. T_i is the initial degradation temperature, $T_{1/2}$ is the temperature of half decomposition, and T_p is the temperature at the maximum rate of weight loss.

In this paper, the weight coefficient C_1, C_2, and C_3 of T_i, T_p, and $T_{1/2}$, are assumed as 7, 2, and 1, respectively, because the initial degradation temperature plays the most important role in fiber thermostability. Therefore, the collecting temperature for each sample can be estimated as shown in Figure 5.

It can be found that the PBO is still the first fiber of the heat-resistant materials in order and the collecting temperature (T_c) in Figure 5 is corresponded with the result of Figure 4.

Generally speaking, the collecting temperature, T_c, can be directly and easily used as an evaluating index to compare the heat-resistance of samples in comprehension.
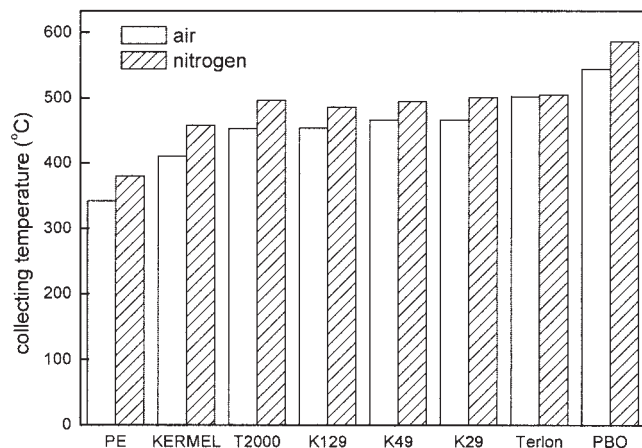
Figure 5 The collecting temperature of thermal degradation in air and N_2 atmosphere.

Thermal degradation kinetics

The comprehensive thermal stability of polymers depends on both various typical temperatures and the apparent activation energy in thermal degradation.[27] So the kinetics of these fibers is developed here.

It is well known that the kinetic procedure and parameters of degradation are important as they affect the degradation rate. The apparent activation energy value, E, of thermodegradation was determined by the Freeman-Carroll method[28] based on the following eq. (2)

$$\frac{d\alpha}{dt} = A \, e^{-E/RT}(1-\alpha)^n \qquad (2)$$

where $\frac{d\alpha}{dt}$ is the degradation rate of weight loss, α is the reacted mass fraction (conversion degree), n is the apparent reaction order, R is the universal gas con-

stant, T is the degradation temperature, and A is the preexponential factor.

According to eq. (2), we have:

$$\ln\left(\frac{d\alpha}{dt}\right) = \ln A - \frac{E}{RT} + n \ln(1-\alpha) \text{ and } d\ln\left(\frac{d\alpha}{dt}\right)$$

$$= -\frac{E}{R}d\left(\frac{1}{T}\right) + nd\ln(1-\alpha)$$

$$\frac{d\ln\left(\frac{d\alpha}{dt}\right)}{d\ln(1-\alpha)} = -\frac{E}{R}\frac{d\left(\frac{1}{T}\right)}{d\ln(1-\alpha)} + n \qquad (3)$$

$$\frac{\Delta\ln\left(\frac{d\alpha}{dt}\right)}{\Delta\ln(1-\alpha)} = -\frac{E}{R}\frac{\Delta\frac{1}{T}}{\Delta\ln(1-\alpha)} + n \qquad (4)$$

Obviously, eqs. (3) or (4) is a linear equation of $y = ax + b$, where y represents $\frac{\Delta\ln(d\alpha/dt)}{\Delta\ln(1-\alpha)}$, a is the slope of the line of $y = ax + b$, x is $\frac{\Delta\left(\frac{1}{T}\right)}{\Delta\ln(1-\alpha)}$, and b is the intercept and equals to n. So the E values can be easily found from the y−x regression line of eqs. (3) or (4). It is mentioned that E are herein calculated within the range of $T_i \pm 10\% \times T_i$.

By using eq. (4) and the measured TG curves, the kinetics parameters, E, n, and the corresponding correlation coefficient, r, of the regression equation can be obtained for each HPF, and the calculated results are shown in Table III. At the same time, the calculation examples of Kevlar®29 under air and nitrogen atmosphere are illustrated in Figure 6 according to the Freeman-Carroll method. From the slope of the fitted straight line, the activation energy (E) value of Kevlar®29 can be found, and from the intercept of the

TABLE III
Kinetic Parameters of Samples Degradation in Air and Nitrogen

Sample	Under air atmosphere			Under nitrogen atmosphere		
	E(kJ/mol)	n	r	E(kJ/mol)	n	r
K29	339.39	0.36	−0.97	320.60	0.37	−0.99
K49	370.80	0.38	−0.99	313.97	0.36	−0.99
K129	320.98	0.35	−0.98	279.48	0.33	−0.99
T2000	259.99	0.45	−0.99	393.82	0.37	−0.98
PBO	107.01	0.26	−0.99	68.74	0.21	−0.98
Terlon®	204.55	0.34	−0.99	414.92	0.42	−0.98
Kermel®	110.11	0.27	−0.78	47.98	0.22	−0.99
UHMW-PE	199.40	0.39	−0.97	213.05	0.41	−0.97

The kinetic parameters of tested samples degradation in air and nitrogen are shown in Table III according to the Freeman-Carroll method. K29 is Kevlar®29; K49 is Kevlar®49; K129 is Kevlar®129; T2000 is Twaron®2000; PE is UHMW-PE. E is the apparent activation energy value; n is the apparent reaction order; r is the corresponding coefficient of the regression equation.
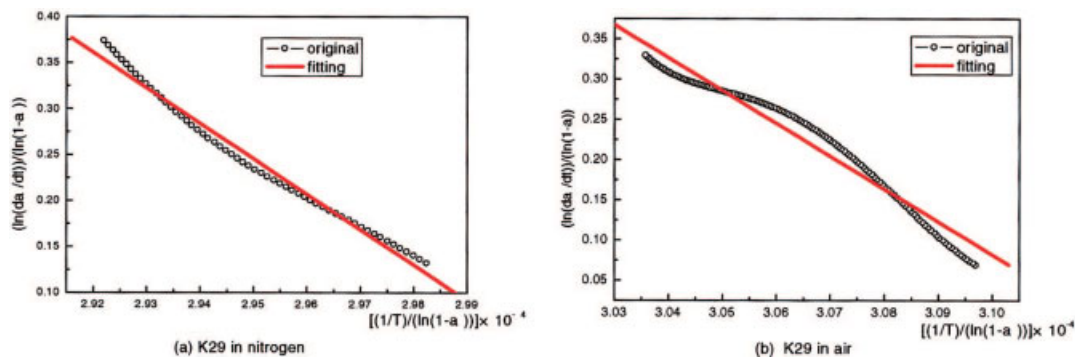
Figure 6 Plots from Freeman–Carroll method. [Color figure can be viewed in the online issue, which is available at www.interscience.wiley.com.]

straight line, the reaction order (n) can also be obtained.

It can be found that the four kinds of *para*-aramids, Kevlar®49, Kevlar®29, Kevlar®129, and Twaron® have similar reaction order (n) and activation energy (E), and the results accord with the shape of TG and DTG curve (Figs. 2 and 3). And the reaction order (n) of the tested three Kevlar® and Twaron® samples in air is near to that in nitrogen. It implies that the reaction mechanism is similar in air and nitrogen atmosphere.

Although the degradation temperature of PBO fiber is the highest, its activation energy is not the highest; only 68.74 KJ/mol under nitrogen atmosphere, whereas about 107.01 KJ/mol in air atmosphere. There is slight difference with that observed in a study by Newell et al.,[21] which probably is due to the different temperature zone chosen. Under nitrogen atmosphere, the activation energy (E) is lower than that in air except for Twaron®2000, Terlon®, and UHMW-PE, of which the values of the activation energies increase in nitrogen. In addition, the reaction order of the three fibers changes much in both atmospheres, for *e.g.*, the reaction order of Twaron®2000 increases from 0.37 (in nitrogen) to 0.45 (in air), while that of Terlon® decreases from 0.42 (in nitrogen) to 0.34 (in air). Combined with the DTG curves shown in Figure 2 and Figure 3, these samples show different shapes from other fibers, which means that the initial thermal degradation mechanism of these samples is different from the other five high performance fibers.

CONCLUSIONS

The TG and DTG results indicate that the thermal stability of the high performance fibers can be characterized with the typical degradation temperatures (T_i, $T_{1/2}$, and T_p). Among the three degradation temperatures, T_i is the most important parameter to evaluate the thermal stability of the fibers. For this reason, we put forward a new parameter, namely the collecting temperature (T_c) to express fiber thermostability more completely and directly, which involves the influencing quantity of the typical degradation temperatures (T_i, T_p, and $T_{1/2}$) on thermal degradation in end usage. The comparison of the measured data to the collecting temperature (T_c), by using the typical degradation temperatures singly or synthetically, is verified that there is a high coincidence between the two sorts of parameters, and the collecting temperature (T_c) represents a more convenient and accurate usage in the evaluation. Therefore, the collecting temperature (T_c) can be directly and easily used as an evaluating index to compare the heat-resistantance of samples.

The typical and the collecting temperatures show that the thermal stability of PBO is the best, Terlon® fiber is the next, Kevlar® and Twaron® fibers are similar, and the Kermel® follows, and the UHMW-PE is the worst whether in nitrogen or air atmosphere treated. Although the TG curves measured in N_2 and air atmosphere are approximately the same, the degradation temperatures in nitrogen are higher than those in air.

From the thermal degradation kinetics of these fibers, it can be found that the four kinds of *para*-aramids, Kevlar®49, Kevlar®29, Kevlar®129, and Twaron® have similar reaction order (n) and activation energy (E) in both air and nitrogen atmosphere. Although the degradation temperature of PBO fiber is the highest, its activation energy is not the highest. The activation energy of initial degradation (E) is closely related with the initial temperature.

References

1. Bourbigot, S.; Flambard, X.; Duquesne, S. Polym Int 2001, 50, 157.

2. Inoue, T.; Komatsu, H.; Yanagi, M. Kobunshi-Ronbunsh 1984, 41, 643.
3. Eashoo, M.; Shen, D.; Wu, Z.; Lee, C. J.; Harris, F. W.; Cheng, S. Z. D. Polymer 1993, 34, 3209.
4. Yang, H. H. Kevlar Aramid Fiber; John Wiley & Sons: New York, 1993.
5. Hearle, J. W. S. High Performance Fibres; Woodhead Publishing Limited: England, 2001.
6. Black, W. B.; Preston, J. High-Modulus Wholly Aromatic Fibers; Marcel Dekker: New York, 1973.
7. Tatsuya, H.; Glyn, O. P. New Fibres; Ellis Horwood Limited: England, 1990.
8. Kwoleck, S. L. U.S. Pat. 3,819,587 (1974).
9. Blades, H. U.S. Pat. 3,869,429 (1975).
10. Powers, E. J.; Serad, G. A. Symposium on the History of High Performance Polymers; American Chem Society: New York, April 15–18, 1986.
11. Marshall, T. U.S. Pat. 4,263,245 (1981).
12. Judge, A.; Montgomery, D. E. Appl Polym Symp 1973, 21, 43.
13. Smith, P.; Lemstra, P. J. U.K. Pat. 2051661 (1979).
14. Davis, H.; Singletary, J.; Srinivasarao, M.; Knoff, W.; Ramasubramanian, M. K. Textil Res J 2000, 70, 945.
15. Dobb, M. G.; Johnson, D. J.; Saville, B. P. J Polym Sci Part B: Polym Phys 1977, 15, 2201.
16. Hindeleh, A. M.; Abdo, Sh. M. Polymer 1989, 30, 218.
17. Brown, J. R.; Ennis, B. C. Textil Res J 1977, 47, 62.
18. Takahashi, Y. Macromolecules 1999, 32, 4010.
19. Wu, Z.; Zhang, A.; Shen, D.; Leland, M.; Harris, F. W.; Cheng, S. Z. D. J Therm Anal 1996, 46, 719.
20. Li, X. G.; Huang, M. R. J Appl Polym Sci 1999, 71, 565.
21. Newell, J. A.; Edie, D. D.; Fuller, E. L., Jr. J Appl Polym Sci 1996, 60, 825.
22. Smith, Q. Using the Perkin Elmer TGA 7; http://www.tmi.utexas.edu/manual_tga.pdf (2004).
23. Burger, C.; Ran, S.; Fang, D.; Cookson, D.; Teramoto, Y.; Cunniff, P. M.; Viccaro, P. J.; Hsiao, B. S.; Chu, B. Polym Preprint 2002, 43, 250.
24. Ward, D. Int Fiber J 2002, 17, 28.
25. Renata, G. K.; Boguslaw, B. J Separ Sci 2003, 26, 1273.
26. Milena, M. C.; Dragan, B.; Renata, J.; Katarina, P. P.; Miroslav, P. Polym Degrad Stabil 2003, 81, 387.
27. Abate, L.; Blanco, I.; Orestano, A.; Pollicino, A.; Recca, A. Polym Degrad Stabil 2003, 80, 333.
28. Freeman, E. S.; Carroll, B. T. J Phys Chem 1958, 62, 394.